Monitoring *B*-site ordering and strain relaxation in $NiFe_2O_4$ epitaxial films by polarized Raman spectroscopy

M. N. Iliev
Texas Center for Superconductivity and Department of Physics, University of Houston, Houston, Texas 77204-5002, USA

D. Mazumdar, J. X. Ma, and A. Gupta
Center for Materials for Information Technology, University of Alabama, Tuscaloosa, Alabama 35487, USA

F. Rigato and J. Fontcuberta
Institut de Ciència de Materials de Barcelona, CSIC, Campus de la UAB, 08193 Bellaterra, Catalunya, Spain
(Received 8 September 2010; published 24 January 2011)

Polarized Raman spectra of $NiFe_2O_4$ (NFO) films of varying thickness and growth temperature are investigated and discussed. We find that the relaxed films obtained at higher temperatures on $MgAl_2O_4$ (MAO) substrate exhibit spectra identical to those of single crystals and provide strong indications for ordering of Ni^{2+} and Fe^{3+} at the octahedral sites. There is evidence for a certain degree of *B*-site ordering even for the thinnest film and the ones grown at the lowest temperature. The variations of Raman mode frequencies and lattice parameters with growth temperature and film thickness provide evidence that the volume of the unit cell decreases under the compressive strain of the NFO film-MAO substrate mismatch. In general, we conclude that the film relaxation and the *B*-site ordering are more sensitive to the growth temperature rather than to the film thickness. Even relatively thin films grown at high temperatures show almost-relaxed lattice parameters and enhanced *B*-site ordering unlike the low-temperature films, which remain strained even when they are thick.

DOI: 10.1103/PhysRevB.83.014108 PACS number(s): 78.30.−j, 68.55.−a, 75.47.Lx

I. INTRODUCTION

The ferrimagnetic spinel oxides, such as MFe_2O_4 (M = Fe,Co,Ni), attract increasing attention as promising candidates for advanced applications such as microwave-integrated devices,[1] magnetoelectric heterostructures,[2] and spin filters.[3] When prepared in the form of thin films, their properties depend on the type of substrate, film thickness, and growth conditions.[4–7] In particular, it was found that very thin films (3–30 nm) of $NiFe_2O_4$ (NFO) may have an enhanced magnetic moment compared to that of the bulk material.[5,6] An enhancement of the magnetic moment has also been observed for 220 nm NFO films deposited at relatively low temperatures on $MgAl_2O_4$ (MAO) substrates, whereas the films deposited under similar conditions on $SrTiO_3$ (STO) substrates exhibit reduced magnetization.[7] It is plausible to expect that the deviation of the properties of the thin films from those of single crystals is related to their structural differences originating from the mismatch between the lattice parameters of the film and substrate, the substitution of *A*-site ions for *B*-site ions, elemental nonstoichiometry, and general lattice disorder due to nonequilibrium growth conditions. Revealing the structural peculiarities of the spinel thin films, however, is to some extent hampered by incomplete knowledge of the real structure of inverse spinels at a microscopic level. Based on the results of neutron diffraction studies,[8,9] there is a consensus that the *averaged* structure of $NiFe_2O_4$ is cubic $Fd\bar{3}m$ (space group No. 227) with the tetrahedral *A* sites (8*a*) occupied by half of the Fe^{3+} cations, whereas the rest of the Fe^{3+} and Ni^{2+} cations are distributed over the octahedral *B* sites (16*d*). There is, however, a fundamental question of whether Fe^{3+} and Ni^{2+} are spread in a random fashion among the *B* sites or whether they exhibit specific short-range order on a spatial scale, which is below the detection limit of the standard diffraction techniques. The symmetry aspects of possible ordering at the *B* sites of inverse spinel structure have been discussed theoretically as early as the 1960s by Haas,[10] but it was only recently pointed out that the polarized Raman spectra provide experimental evidence for such ordering.[11] Indeed, the $NiFe_2O_4$ single crystals exhibit a much richer Raman spectra with polarization properties different from these expected for an $Fd\bar{3}m$ structure. The larger number of Raman lines and their polarization dependence, however, can consistently be explained by the ordering of Ni^{2+} and Fe^{3+} at the *B* sites resulting in the coexistence of uniformly distributed twin variants of tetragonal $P4_122$ and/or orthorhombic $Imma$ structure.[11] In this study, we show that the Raman spectra of NFO single crystals and relaxed thin films are identical, and therefore the *B*-site ordering and microtwinning are also characteristic for an "ideal" NFO thin film. Based on this finding, we use the Raman spectra of NFO films to analyze the evolution of the film microstructure with growth conditions, postannealing, and thickness.

II. SAMPLES AND EXPERIMENT

We studied two sets of (001)-oriented NFO/MAO films prepared by different techniques. The first set, denoted as NFO-*A*, has been deposited by pulsed laser deposition (PLD) at substrate temperatures of 175, 250, 325, 400, 550, and 690 °C under ozone/oxygen pressure of 10 mTorr, the film thickness being ≈ 220 nm. The second set, denoted as NFO-*B*, has been grown by rf magnetron sputtering at a substrate temperature of 600 °C under a mixed atmosphere of O_2 and Ar (1:10 gas flux ratio) at 250 mTorr pressure. NFO-*B* films of thicknesses 6.5, 13.4, 29, and 69 nm were studied. More details on the preparation and characterization of NFO-*A* and

NFO-B films can be found in Refs. 7 and 6, respectively. We will only mention here that the films of the NFO-A series appear to gradually relax, with cell parameters approaching the bulk values, with increasing deposition temperature; the same trend is observed in the films of series B with increasing film thickness. The single crystals of NFO used for comparison are described in Ref. 11. From our measurements we find no difference related to the growth technique used (PLD vs rf sputtering).

The Raman spectra were measured at room temperature with XX, XY, $X'X'$, and $X'Y'$ backward-scattering configurations using a T64000 spectrometer equipped with a microscope and a liquid-nitrogen-cooled charge-coupled device (CCD). The first and second letter in configuration notations denote the polarization of the incident and scattered light, respectively, along the $X \equiv [100]_c$, $Y \equiv [010]_c$, $X' \equiv [110]_c$, and $Y' \equiv [1\bar{1}0]_c$ cubic directions. In the spectra of thinner NFO-B films the Raman signal from the MAO substrate was superimposed. The substrate signal was eliminated by measuring the MAO spectra in the same scattering configuration and subtracting them from the combined NFO-B + MAO spectra.

III. RESULTS AND DISCUSSION

From symmetry considerations one expects five Raman-active modes for the spinel $Fd\bar{3}m$ structure, $A_{1g} + E_g + 3F_{2g}$. The A_{1g} mode is allowed with XX, but forbidden with $X'Y'$ and XY scattering configurations. It corresponds to stretching (breathing) vibrations of oxygens against Fe^{3+} in FeO_4 tetrahedra, which presupposes that its frequency is the highest of the Raman modes. The E_g mode also contains only oxygen motions, but they are of bending type and its frequency is lower. The E_g mode is allowed with XX and $X'Y'$ configurations and forbidden in the XY spectra. As for the F_{2g} modes, they involve motions of both oxygen and A-site atoms, allowed in the XY spectra and forbidden in the XX and $X'Y'$ spectra.

The XX, $X'Y'$, and XY spectra of NFO single-crystal and relaxed NFO-A (220 nm, 690 °C) and NFO-B (69 nm, 600 °C) films are compared in Fig. 1. The spectra of the relaxed NFO-A and NFO-B films are practically identical to those of the NFO single crystal. The number of Raman peaks, however, is larger than expected for a spinel $Fd\bar{3}m$ structure. In particular, with XX scattering configuration where only one A_{1g} and one E_g mode are expected, there are seven clearly pronounced bands at 333, ≈450, 487, 571, 591, ≈660, and 703 cm^{-1}. Of these, the 333 cm^{-1} peak exhibits E_g-type symmetry as it is pronounced also in the $X'Y'$ spectra, but not in the XY spectra, whereas the 703 cm^{-1} has the characteristics of an A_{1g} mode. Of the peaks seen in the XY spectra, only the one at 213 cm^{-1} has clear F_{2g} symmetry.

The presence of additional peaks is consistent with the ordering of Ni^{2+} and Fe^{3+} at the B sites, resulting in the coexistence of uniformly distributed twin variants of tetragonal $P4_122$ and/or orthorhombic $Imma$ structure.[11] Alternatively, these spectral features have been attributed to the activation of otherwise forbidden phonon modes due to cationic disorder and/or nonstoichiometry.[12–15] The variation of the Raman spectra of NFO films with substrate temperature and film thickness provide additional arguments in favor of or against these conflicting models.

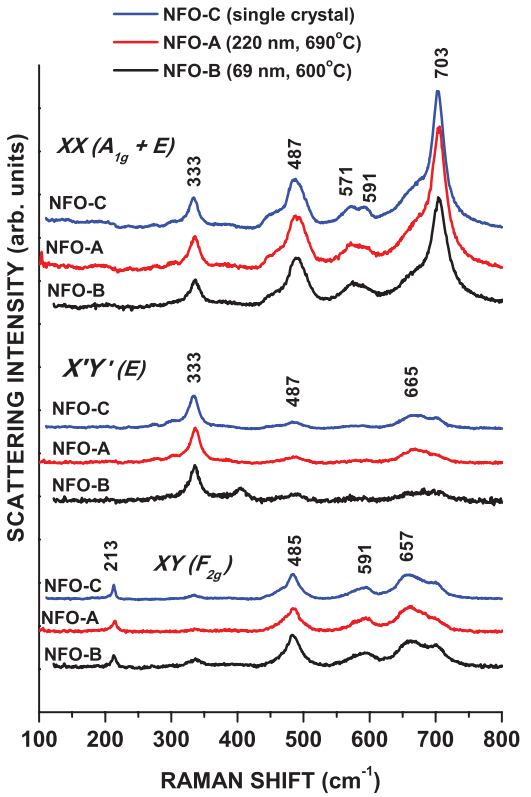

FIG. 1. (Color online) Polarized Raman spectra of $NiFe_2O_4$ single-crystal (NFO-C) and relaxed NFO-A and NFO-B thin films as obtained at 300 K with 488 nm excitation.

A. Effect of substrate temperature on the Raman spectra of NFO films

The Raman spectra of NFO-A films grown at different substrate temperatures are compared in Fig. 2. Their variations with scattering configurations clearly indicate that all films are epitaxial. The Raman lines of the spectra of films grown at lower temperatures are somewhat weaker, broader, and as a rule, shifted to higher wave numbers as compared to single-crystal values (see Fig. 3). The number of Raman peaks is larger than expected for the spinel structure, which indicates that the additional modes are either disorder activated or due to partial ordering resulting in local structure(s) of lower symmetry.

The structural disorder, if present, could be caused by (i) oxygen nonstoichiometry, (ii) Ni^{2+} for Fe^{3+} partial substitution at the tetragonal A sites, or (iii) Ni^{2+}/Fe^{3+} disorder at the B sites resulting in disorder of the oxygen sublattice.

Indications for the substitution of Ni^{2+} for Fe^{3+} at the A sites could be found only for the 175 °C film, namely, in the softening of the high-frequency A_{1g}-type mode compared to 250 and 325 °C films (Fig. 3). The A_{1g}-type mode near 710 cm^{-1} corresponds to stretching (breathing) vibrations of AO_4 tetrahedra. The force constant k, which governs the mode frequency ($\omega^2 \propto k/m$) is determined by the charges Z_A and Z_O of the central ion A and oxygens, respectively,

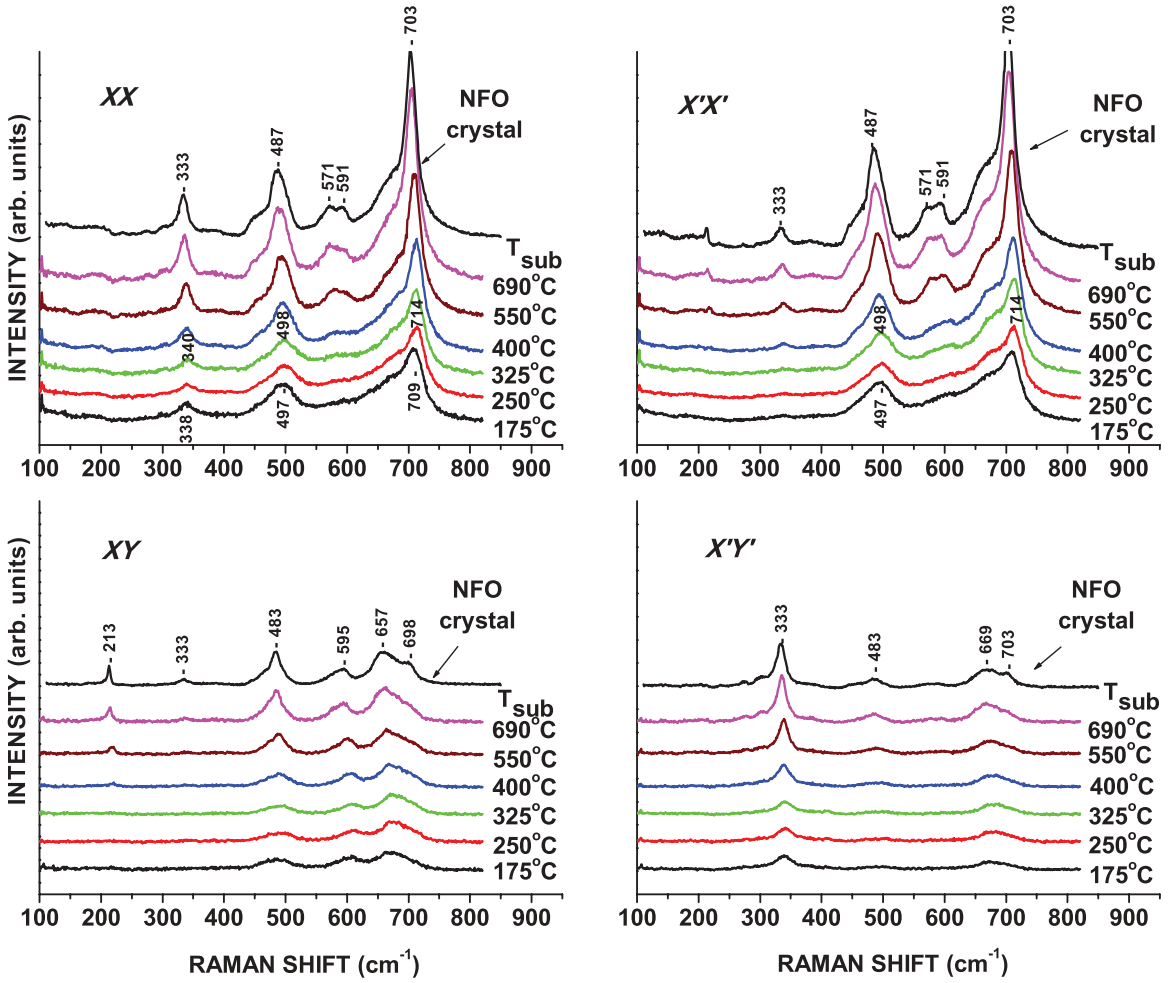

FIG. 2. (Color online) Polarized Raman spectra of NFO-*A* thin films prepared at various temperatures of the MAO substrate. The spectra of $NiFe_2O_4$ single crystals (NFO-*C*) are also shown. All spectra are obtained at 300 K with 488 nm excitation.

and by the cation-oxygen distance $r_{A\text{-}O}$, as $k \propto Z_A Z_O / r^3_{A\text{-}O}$. The replacement of Fe^{3+} (ionic radius 0.49 Å) by Ni^{2+} (ionic radius 0.55 Å) would decrease the mode frequency due to both $Z_{Ni^{2+}} < Z_{Fe^{3+}}$ and $r_{Ni\text{-}O} > r_{Fe\text{-}O}$. We note here that the mode softening could also be caused by oxygen nonstoichiometry or by the fact that partial Ni for Fe substitution at tetragonal sites results in extra disorder of the oxygen sublattice, which may affect more modes in a similar way. Partial Ni^{2+} for Fe^{3+} substitution at the *A* sites, however, is likely negligible for the films grown at substrate temperatures of 250 °C and higher.

To analyze possible oxygen nonstoichiometry of the films grown at lower substrate temperatures the following experiment was conducted. NFO-*A* film grown at 250 °C was cut into three pieces. One of these pieces was postannealed for eight hours at 900 °C in air, and another in inert (argon) atmosphere. The corresponding Raman spectra of the original and postannealed films were then measured under identical experimental conditions. The comparison of the spectra (Fig. 4) shows that both types of postannealing have the same effect: the spectra become practically identical to those of stoichiometric NFO single crystals and relaxed NFO-*B* films. The reasonable conclusion is that the starting oxygen content even for films grown at low substrate temperatures is close to the stoichiometric one and the thermal treatment keeps it intact. Obviously, the annealing-induced changes of spectra reflect changes of the local film structure at a fixed elemental content.

The variations of the Raman spectra with substrate temperature are consistent with ordering proceeding in two steps: first involving separation into tetrahedral and octahedral sites for $T_{sub} < 250$ °C, and then at octahedral sites for $T_{sub} > 250$ °C. Given that the cation substitution at the *A* sites and oxygen deficiency are negligible, the difference between the Raman spectra of the films obtained at lower and higher substrate temperatures is most likely caused by the arrangement of the Ni^{2+} and Fe^{3+} ions over the *B* sites. Indeed, in the case of low-temperature films, the surface diffusion, which is important for cation (and anion) ordering, is either totally quenched or very slow. Therefore, it is plausible to assume that the low-temperature films have a higher degree of cation disorder compared to the high-temperature films. Much faster surface diffusion at elevated temperatures during the film growth makes it possible to reach the state of minimum total energy. DFT calculations of possible cation arrangements have shown that the *B*-site ordering in ...-Ni^{2+}- Fe^{3+}-Ni^{2+}- Fe^{3+}-Ni^{2+}-Fe^{3+}-... chains along the [110] and [1$\bar{1}$0] cubic directions is

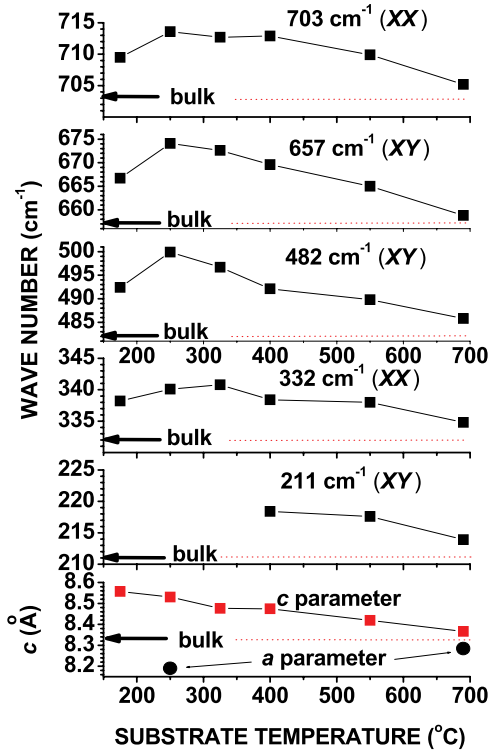

FIG. 3. (Color online) Variations of the phonon frequencies and in-plane a and out-of-plane c parameters of NFO-A as a function of substrate temperature during film growth.

energetically most favorable.[16] This type of ordering results in a local structure of tetragonal $P4_122$ symmetry with a larger primitive cell and therefore a larger number of Raman-allowed modes. Upon film growth or cooling after postannealing, the tetragonal axis may be aligned along each of the equivalent a_c, b_c, or c_c cubic directions; therefore, one expects heavy microtwinning resulting in averaged cubic structure.

From symmetry considerations some of the Raman modes of $P4_122$ directly correspond to Γ-point modes of $Fd\bar{3}m$, whereas the rest of the modes originate from a zone folding, which maps the zone-boundary X point of $Fd\bar{3}m$ onto the Γ point of $P4_122$. Such are, for example, the components of the A_1-B_2 pairs near 570–595 cm^{-1}, which could be used as markers for the presence of B-site ordering.[11] As follows from Fig. 2, these features become more pronounced at substrate temperatures above 500 °C, which provides evidence for a high degree of B-site ordering in the films prepared under these growth conditions.

The NFO-A films, although relatively thick (220 nm), remain unrelaxed when grown at low temperatures indicating that the thermal energy is not high enough to induce plastic deformations of the lattice. This results in significant variations of the quasicubic lattice parameters, as illustrated in the bottom panel of Fig. 3, where the dependence of the out-of-plane c parameter and in-plane a parameter as a function of the substrate temperature is shown.

B. Effect of film thickness on the Raman spectra of NFO/MAO films

The NFO-B films have been prepared at 600 °C, a temperature high enough for surface diffusion resulting in B-site ordering. The comparison of Raman spectra of films of different thickness allows one to separate the effect of substrate/film mismatch from that of lattice disorder. As follows from Fig. 5, the structure near 570–590 cm^1 in the XX spectra, which indicates a high degree of B-site order, is present even in the thinnest film studied (6.5 nm). The most significant effect of decreasing film thickness is the

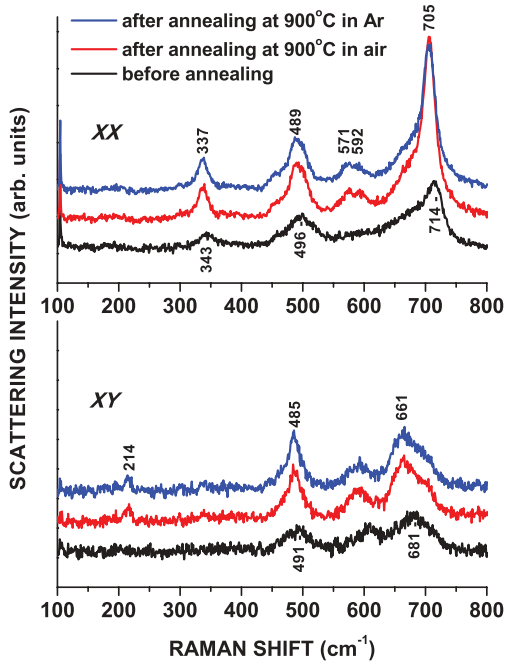

FIG. 4. (Color online) Raman spectra of NFO-A film grown at 325 °C before and after postannealing in air or Ar.

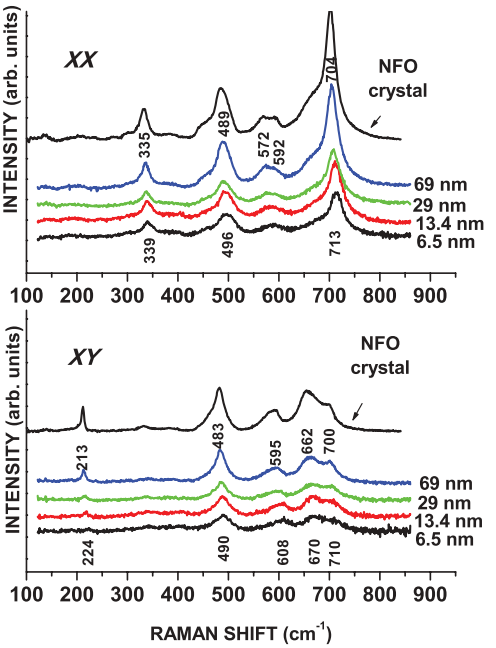

FIG. 5. (Color online) Raman spectra of NFO-B films of various thicknesses. The spectra of NFO single crystals are also shown for comparison.

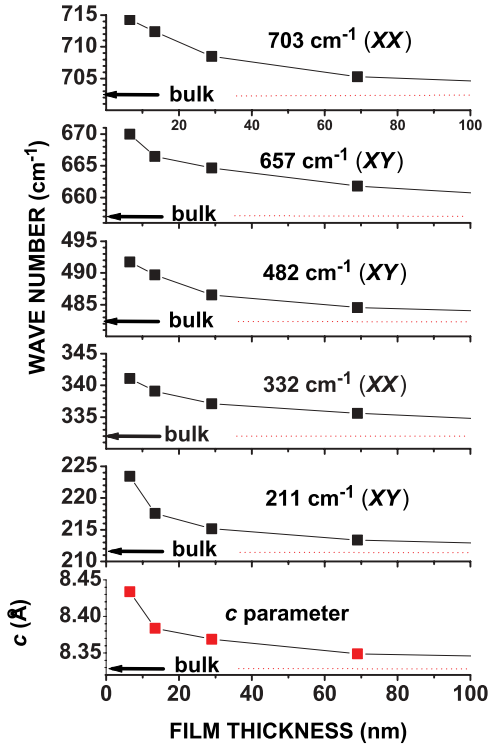

FIG. 6. (Color online) Variations of the phonon frequencies and out-of-plane c parameter of NFO-B as a function the film thickness.

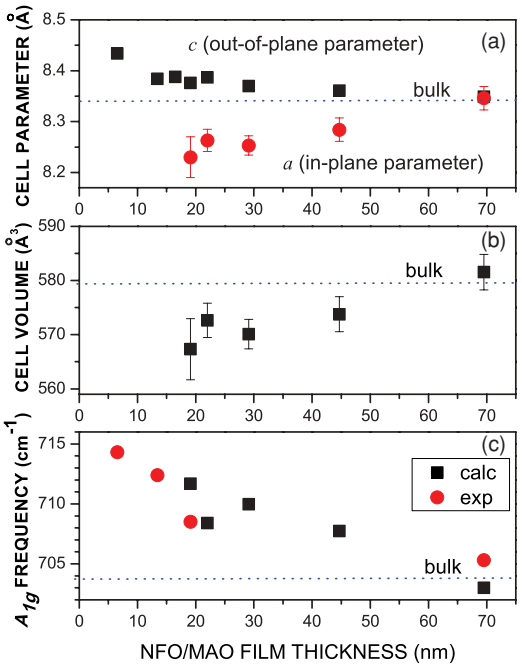

FIG. 7. (Color online) Variations with NFO-B film thicknesses of (a) cell parameters, (b) cell volume, and (c) calculated and experimental A_{1g}-like mode frequency.

hardening of all Raman modes (see Fig. 6). Such hardening can be explained by the fact that the in-plane compression of the unit cell is not fully compensated by its out-of-plane extension, i.e., the volume of the strained cell is smaller than that of the relaxed unit cell, as illustrated in Fig. 7. Here we could analyze the dependence on the cell volume of the frequency of the A_{1g}-type mode at 705–715 cm^{-1}, corresponding to the stretching (breathing) vibrations of AO_4 tetrahedra along the cubic {111} directions. A reasonable assumption is that the A-O bond lengths scale with the length of the {111} space diagonals d and the mode frequency will increase with decreasing d and vice versa following the relation $\omega \propto d^{-3/2} = (2a^2 + c^2)^{-3/4}$, where a and c are the in-plane and out-of-plane lattice parameters, respectively. The A_{1g}-type mode frequency will therefore vary with a and c as

$$\omega = \omega_0 \frac{3^{3/4} a_0^{3/2}}{(2a^2 + c^2)^{3/4}}, \qquad (1)$$

where ω_0 and a_0 are the mode frequency and the lattice constant of the bulk NFO, respectively.

The comparison of c-parameter dependencies on the substrate temperature (Fig. 3) and film thickness (Fig. 6) clearly show that the relaxation mechanism, and therefore the lattice parameters, are less sensitive to the thickness rather than growth temperature. Even relatively thin higher-temperature NFO-B films show almost-relaxed lattice parameters, unlike the low-temperature NFO-A films, which remain strained even if they are thick.

The variations in the Raman spectra of NFO-B films with decreasing film thickness do not support the previous assumption that the enhanced magnetization of very thin NFO films may be due to partial substitution of Ni^{2+} for Fe^{3+} at the A sites.[6] Enhancement of the magnetic moment, however, has been observed in small size ferrite particles[17] and it has been attributed to a frustration of collinear spin arrangement due to surface effects. It is conceivable that a similar scenario in nanometric thin films could lead to an enhanced magnetization.

Recently, controversial conclusions on the strain effect in thin films of inverse spinel ferrites have been made on the basis of experimental and theoretical studies of Poisson ratio $\nu = -\epsilon_l/\epsilon_t = -(c - a_0)/(a - a_0)$, where a and c are the in-plane and out-of-plane lattice parameters, respectively, of the thin-film material and a_0 is the corresponding lattice parameter in the bulk. While Valant *et al.*[18] reported a *negative* value of $\nu \approx -0.85$ for 25–100 nm films of $CoFe_2O_4$ (CFO) films on $SrTiO_3$ (STO) substrate (which means that both in-plane and out-of-plane parameters shrink under compressive strain), Fritsch and Ederer[19] predicted normal *positive* $\nu \approx 1.2$ for both compressively strained NFO and CFO. Our results [see Fig. 7(a)] clearly show a thickness-dependent *positive* Poisson ratio for NFO/MAO films with ν ranging between 0.7 for $d = 20$ nm and ≈ 0 for $d = 70$ nm. Similar results have been obtained for CFO/MAO films.[20] All this puts in question the statement in Ref. 18 that a negative Poisson ratio (if any) results from the characteristic atomic arrangement of the spinel structure and should be a general effect.

IV. CONCLUSIONS

Raman spectroscopy has been applied to characterize the structure of $NiFe_2O_4$ thin films grown on $MgAl_2O_4$ substrates as a function of substrate temperatures between 175 and 690 °C and film thicknesses between 6.5 and 69 nm. It has been found that the structure is characterized by the ordering of Ni and Fe

at the *B* sites and the absence of Ni at the *A* sites, even for the thinnest films. These results indicate that the magnetization enhancement previously observed[5,6] for very thin NFO films cannot be attributed to partial inversion of the spinel structure, but more subtle effects, including interface effects, may play a role. The variation of the phonon frequencies is consistent with the experimentally confirmed decrease of the unit-cell volume under compressive strain. The comparison of Raman and structural data for the two sets of films clearly shows that the relaxation mechanism, and therefore the lattice parameters, are more sensitive to the growth temperature rather than the thickness. Even relatively thin NFO-*B* films grown at higher temperatures exhibit almost-relaxed lattice parameters unlike the low-temperature NFO-*A* films, which remain strained even if they are thick.

ACKNOWLEDGMENTS

The help of K. Sasmal in postannealing and H. Sato in x-ray experiments is greatly acknowledged. This work is supported in part by the State of Texas through The Texas Center for Superconductivity at the University of Houston. The work at the University of Alabama was supported by ONR under Grant No. N00014-09-1-0119.

[1] J. D. Adams, S. V. Krishnaswamy, S. H. Talisa, and K. C. Yoo, J. Magn. Magn. Mater. **83**, 419 (1990).
[2] Yi Zhang, Chaoyong Deng, Jing Ma, Yuanhua Lin, and Ce-Wen Nan, Appl. Phys. Lett. **92**, 062911 (2008).
[3] U. Lüders, A. Barthélémy, M. Bibes, K. Bouzehouane, S. Fusil, E. Jacquet, J. P. Contour, J. F. Bobo, J. Fontcuberta, and A. Fert, Adv. Mater. **18**, 1733 (2006).
[4] C. N. Chinnasamy, S. D. Yoon, A. Yang, A. Baraskar, C. Vittoria, and V. G. Harris, J. Appl. Phys. **101**, 09M517 (2007).
[5] U. Lüders, M. Bibes, J.-F. Bobo, M. Cantoni, R. Bertacco, and J. Fontcuberta, Phys. Rev. B **71**, 134419 (2005).
[6] F. Rigato, S. Estradé, J. Arbiol, F. Peiró, U. Lüders, X. Martí, F. Sánchez, and J. Fontcuberta, Mater. Sci. Eng. B **144**, 43 (2007).
[7] J. X. Ma, D. Mazumdar, G. Kim, H. Sato, N. Z. Bao, and A. Gupta, J. Appl. Phys. **108**, 063917 (2010).
[8] J. M. Hastings and L. M. Corliss, Rev. Mod. Phys. **25**, 114 (1953).
[9] K. N. Subramanyam, J. Phys. C **4**, 2266 (1971).
[10] C. Haas, J. Phys. Chem. Solids **26**, 1225 (1965).
[11] V. G. Ivanov, M. V. Abrashev, M. N. Iliev, M. M. Gospodinov, J. Meen, and M. I. Aroyo, Phys. Rev. B **82**, 024104 (2010).
[12] P. R. Graves, C. Johnston, and J. J. Campaniello, Mater. Res. Bull. **33**, 1651 (1988).
[13] Z. H. Zhou, J. M. Xue, J. Wang, H. S. O. Chan, T. Yu, and Z. X. Shen, J. Appl. Phys. **91**, 6015 (2002).
[14] M. A. Laguna-Bercero, M. L. Sanjuàn, and R. I. Merino, J. Phys.: Condens. Matter **19**, 186217 (2007).
[15] W. H. Wang and X. Ren, J. Cryst. Growth **289**, 605 (2006).
[16] D. Mazumdar (unpublished).
[17] R. N. Bhowmik and R. Ranganathan, Solid State Commun. **141**, 365 (2007).
[18] M. Valant, A.-K. Axelsson, F. Aguesse, and N. M. Alford, Adv. Funct. Mater. **20**, 644 (2010).
[19] D. Fritsch and C. Ederer, Phys. Rev. B **82**, 104117 (2010).
[20] J. Fontcuberta (unpublished).